INDIAN JOURNAL OF SCIENCE AND TECHNOLOGY

RESEARCH ARTICLE

PV Based Single Stage Cascaded Seven Level Modular Multilevel Converter with ZSV Control for Grid Interfaced System

P Ananiya[1], **R Pazhanimurugan**[2]*, **K Kalpana**[3], **M Nivedha**[3]

1 PG Scholar, Department of Electrical and Electronics Engineering, Arasu Engineering College, Affiliated to Anna University, Tamil Nadu, India
2 Associate Professor, Department of Electrical and Electronics Engineering, Arasu Engineering College, Affiliated to Anna University, Tamil Nadu, India
3 Assistant Professor, Department of Electrical and Electronics Engineering, Arasu Engineering College, Affiliated to Anna University, Tamil Nadu, India

OPEN ACCESS

Received: 15-06-2024

Accepted: 27-09-2024

Published: 15-10-2024

Citation: Ananiya P, Pazhanimurugan R, Kalpana K, Nivedha M (2024) PV Based Single Stage Cascaded Seven Level Modular Multilevel Converter with ZSV Control for Grid Interfaced System. Indian Journal of Science and Technology 17(39): 4073-4083. https://doi.org/10.17485/IJST/v17i39.1975

* **Corresponding author**.

rpmuruganmail@gmail.com

Funding: None

Competing Interests: None

Published By Indian Society for Education and Environment (iSee)

ISSN
Print: 0974-6846
Electronic: 0974-5645

Abstract

Objectives: Climatic perturbation and environmental factors affect solar power generation. When these solar panels are connected to the grid it causes power quality issues such as voltage harmonics, voltage distortion, etc. These problems are addressed in this paper using a distributed MPPT algorithm. **Methods**: Multilevel inverters have made remarkable contributions to renewable energy, high voltage, and other high-power applications. Hence, a single-stage Cascaded Seven-Level Modular Multilevel Converter (CSLMMC) is used to address the issues. Zero Sequence Voltage (ZSV) control is proposed for producing balanced power during varying irradiance conditions. The proposed method is simulated using MATLAB SIMULINK software. Partial shading is conquered by using distributed MPPT. **Findings**: The simulation of the proposed system is performed for a three-phase system. The three-phase Cascaded Modular Multilevel Converter is connected to the grid through two loads which are controlled by a Zero Sequence Voltage Controller. Power quality parameters such as current, harmonics, and power are analyzed for the proposed system. **Novelty**: THD analysis for a five-level cascaded H bridge converter and the proposed systems are compared and presented.

Keywords: Photo voltaic; Cascaded seven-level modular multilevel converter; Zero sequence control; Maximum power point tracking; Voltage Source Converter

1 Introduction

Solar photovoltaic (PV) energy generation systems are becoming more popular, as a part of this Global PV expansion is going to increase rapidly due to the improvements in power electronic technologies and the cost reduction of the PV modules, making PV systems an attractive solution for a cheap energy source that can be constructed and enter into service in less than 1 year. It has been reported by the International Renewable

Energy Agency (IRENA)in 2020 that the average price of PV modules has been reduced by around 85% in the last decade. The price has been reduced by 13% in 2019 only to around 5p per 1 kWh. Recently, as of 2021, the global solar PV capacity was estimated to be over 550 GW [1]. Based on the number of power processing stages PV inverters can be put under two different categories, two-stage inverters and single-stage inverters (SSI). In two-stage inverters at the initial stage, PV array output is increased to a higher level with the help of a DC-DC boost converter while tracking maximum solar power, and during the second stage, this DC is converted into AC power of high quality [2].

The design and frequency control of a seven-level H-bridge multilevel converter is carried out for the grid integration of a large photovoltaic (PV) system without a bulky line transformer, as the multilevel converter provides direct integration to the medium voltage grid [3]. A wide range of research has been done by the research community on different types of multilevel inverter topologies. Various basic multilevel inverter topologies have been discussed [4]. Modular Multilevel Converter (MMC) has attracted interest from the research community for its abundant advantages such as the ability to control the power flow, easy implementation, low harmonic distortion in the output voltage, and lower maintenance cost [5]. To improve the power quality of multilevel inverters, several modulation techniques have been proposed. The amount of conduction and switching losses of a multilevel inverter circuit greatly depends upon the switching technique used in the multilevel inverters [6].

The reduced number of levels of 2L-VSCs causes loss problems and poor power quality due to their bad harmonic profile. To solve this issue, the modular multilevel converter (MMC) has drawn the attention of both industry and academic sectors due to its capability to generate sinusoidal voltages and currents with a low content of harmonic distortions at the load side [7]. Among these MMC topologies, the cascade H-Bridge (CHB) is a popular choice because of its modularity, which simplifies the extension for a higher number of levels of the MMC. Moreover, the MMC does not demand a vast number of flying capacitors or clamping diodes. Consequently, the CHB-based MMC is currently a competitive choice in the new era of VSCs MMIs provide the required modularity and scalability, which means that a large-scale PV system can generate high power with smaller semiconductor devices [8]. The structure of the converter in the proposed system is modular in nature, in case of a faulty condition that particular cell alone can be detached and the other cells can be operated normally. The switches of the converter undergo less voltage stress as they operate for a certain period.

2 Methodology

2.1 Cascaded

Modular Multilevel Converter

The cascaded Seven Level Modular Multilevel Converter (CSLMMC) is comprised of a series of cascaded H-bridge cells with separate PV array for each cell. Cascaded MMC topologies have many attractive features, which make them promising for employment in large-scale PV applications. In Cascaded MMC, the inputs of the H-bridges are connected to several PV arrays to provide the required modularization. Each H-Bridge cell has four switches and is fed by a solar array with a maximum power capability of 240W.

The three-phase grid-connected cascaded H-bridge multilevel PV inverter is analyzed wherein the PV array is directly connected to each H-bridge cell to gather the maximum amount of available power, and the PV string is operated at MPPT voltage. DC source for each H – bridge is formed by connecting PV arrays in series. This manner of connection can improve solar PV systems' efficiency because each PV string operates independently [9], with its control and consequently better MPPT performance can be obtained. Decentralized maximum-power-point trackers are recommended to solve the partial shading effect.

2.2 Maximum Power Point Tracking

The basic principle of several MPPT approaches relies on the observation of variations in currents and voltages that occur because of pulsations in instantaneous power. The slope of the PV array power-voltage curve is zero at MPP [10]. This fact is used in incremental conductance algorithms to track MPP. As the operating point moves towards the left of MPP the slope becomes positive and when the operating point moves right of MPP value of the slope becomes negative. The tracking algorithm determines the output by taking the derivative of the power and voltage of the PV panel. This method is in accordance with a property that the slope of the PV array is zero at MPP, presented as

$$\frac{\delta Ppv}{\delta Vpv} = 0 \tag{1}$$

where P_{PV} is the PV module output power and V_{pv} is the PV module voltage.

The unbalances formed inside the phases of the converter are suitably handled by the MPPT algorithm. The conditions of the algorithm for tracking maximum power are given as [11],

$$\frac{\triangle I_{pv}}{\triangle V_{pv}} = -\frac{I_{pv}}{V_{pv}}\, if\ P_{PV} = MPP \tag{2}$$

$$\frac{\triangle I_{pv}}{\triangle V_{pv}} > -\frac{I_{pv}}{V_{pv}}\, if\ P_{PV} < MPP \tag{3}$$

$$\frac{\triangle I_{pv}}{\triangle V_{pv}} < -\frac{I_{pv}}{V_{pv}}\, if\ P_{PV} > MPP \tag{4}$$

Maximum power is accomplished by constantly differentiating the instantaneous and incremental conductance values. Existing literature has global MPPT, where only one MPPT is used in total, which leads to reduced PV power generation during partial shading conditions. Distributed MPPT provides maximum power extraction from each PV panel efficiently under partial shading conditions. Also, Distributed MPPT helps produce balanced power output from PV panels within the phase. It reduces the possibility of mismatch issues in voltage and current levels during partial shading conditions and increases the energy captured by 20%. Distributed MPPT increases the cost of the system as individual MPPT is added to each PV panel but it provides improved overall PV power generation.

2.2.1 Partial Shading

The MPPT controller directs the operation of the PV modules on the maximum power point (MPP) which is the maximum operation point on the power-voltage (P–V) curve, making an allowance for the maximum quantity of PV module power to be generated as revealed in Figure 1. To obtain this maximum power from the PV module, the PV module current and voltages should be kept at point B on the current-voltage (I–V) curve so the power is kept at point D on the P–V curve.

The PV curves change with the varying solar irradiance and temperature. Therefore, the MPPT controllers should avoid settling at the local maxima points instead of the global maximum, which puts an additional burden on the operation. As the P–V curve has several peak points during partial shading conditions, controllers may fail to find the maximum peaks to acquire the highest MPP and they usually settle at a local MPP resulting in up to 70% power loss. New advanced MPPT control strategies have been developed later to deal with the efficiency degradation and sluggish tracking speed under partial shading conditions. These strategies aim to solve the partial shading problems, deal with minor steady-state oscillations, reduce the disturbance around MPP, provide flexibility when operating with nonlinear loads, and provide a high degree of accuracy. A unified control using a Cascaded Fuzzy Logic Controller (CFLC) is proposed for both the maximum power point tracking and Modular 7 Level Converter (M7LC) control. The CFLC is analogized with the conventional PI and Fuzzy controllers under both normal and partially shaded conditions [12]. Figure 1 shows partial shading effects on P-V and I-V curves.

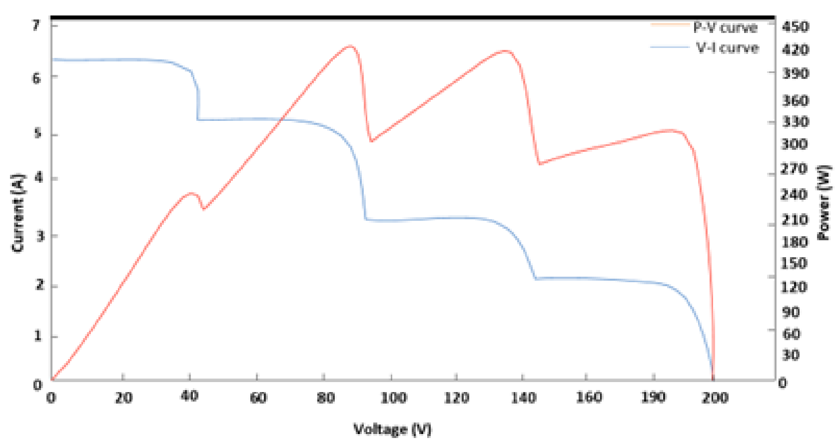

Fig 1. Partial shading effects on P-V and I-V curve

The power output during partial shading is complex to conclude. Hence analysis has been done for measuring partial shading, the phenomenon based on the Lambert model as shown by the equations below

$$V = (Iph + Is)(Rsh - (Rs + Rsh)I - a * Lambert(W) \tag{5}$$

$$W = \frac{Rsh \times Is}{a} e^{\left(\frac{Rsh((Iph+Is)}{a}\right)} \tag{6}$$

2.2.2 Distributed MPPT

Differences in temperature, insolation, manufacturing tolerance, aging, etc. will lead to a mismatch between PV modules. Regardless of the cause of the mismatch, this situation manifests as an asymmetry in the current voltage (i—v) characteristics of PV modules. Thus, since some of the PV modules within a PV string exhibit different i – v characteristics from others, it is impossible to find an operation point at which all the modules in the string operate at the MPP. The intermittent nature of PV arrays introduces a power unbalance inside the converter, which affects its operation[13]. Power electronics-based power processing schemes in distributed MPPT systems are highlighted[14]. It is mainly used to handle the partial shading effect. The distributed MPPT facilitates the extraction of maximum power from each module, thus eliminating the mismatch losses. The advantages of distributed MPPT[15] over the conventional MPPT have more impacts on partial shading and other mismatch issues. The proposed distributed MPPT technique determines the peaks of the power during unbalances effectively. MPPT is used in each of the PV outputs to maintain the same voltage at partial shading.

2.3 Control scheme of the proposed system

The main purpose of the PV systems controllers is to control the PV converters, so the DC energy generated by PV modules is converted to AC power and injected into the AC electrical grid. The controller ensures that the energy harvested from the DC side is maximized and that the power delivered at the output side is improved in terms of power quality and the grid's standards[16]. This desired operation is dependent on developing a rapid and accurate control system. Therefore, the control process is not less important than the electronic power topology itself. The control system of the grid-connected inverters can be classified into two main parts. The first is the MPPT controller, on the input side, which deals mainly with the PV modules. This controller is responsible for extracting maximum power from the PV modules and ensuring that they are operating according to the specifications determined by their manufacturer. The second part is a grid-side inverter controller, which regulates the power transfer process and ensures that output voltages and currents are within the acceptable ranges set by the grid's codes.

2.3.1 Main Controller

The main controller of the proposed system consists of a) MPPT, b) active and reactive current references, and c) a feed-forward decoupling control structure.

The foremost level is to feed the power and current from PV panels to MPPT and can be presented as

$$P_{pvk} = V_{pvk} * i_{pvk} \tag{7}$$

where P_{pvk} is the power extracted from PV and fed to the MPPT controller. k value varies from 1 to 9 as there are nine PV Panels connected in our converter circuitry. The output from the MPPT controller is mathematically given as

$$\Sigma V^*_{MPPr} = V^*_{MPP1} + V^*_{MPP2} + V^*_{MPP3} \tag{8}$$

$$\Sigma V^*_{MPPy} = V^*_{MPP4} + V^*_{MPP5} + V^*_{MPP6} \tag{9}$$

$$\Sigma V^*_{MPPb} = V^*_{MPP7} + V^*_{MPP8} + V^*_{MPP9} \tag{10}$$

Now the summation of all the PV and MPPT voltages are

$$V^*_{MPP} = \Sigma V^*_{MPPr} + \Sigma V^*_{MPPy} + \Sigma V^*_{MPPb} \tag{11}$$

$$V_{pv} = \Sigma V_{pvr} + \Sigma V_{pvy} + \Sigma V_{pvb} \tag{12}$$

Where,

$$\Sigma V_{pvr} = V_{pv1} + V_{pv2} + V_{pv3} \tag{13}$$

$$\Sigma V_{pvy} = V_{pv4} + V_{pv5} + V_{pv6} \tag{14}$$

$$\Sigma V_{pvb} = V_{pv7} + V_{pv8} + V_{pv9} \tag{15}$$

The sum of the output of the MPPT module V_{MPP} and PV module V_{pv} is differentiated and transferred to the PI controller to generate an error signal.

$$Error\ signal = K_p\left(\Sigma V_{pv} - \Sigma V^*_{MPP}\right) + K_I \int \left(\Sigma V_{pv} - \Sigma V^*_{MPP}\right) \tag{16}$$

which is then compared with d-q axis currents**.** A reference d-q axis is generated by current controllers. The proportional-integral (PI) controllers have transfer functions G_{vd}, G_{id} and $G_{iq}$for current and voltage loops. The angle for the abc to dq reference frame is given by

$$\begin{bmatrix} a \\ b \\ c \end{bmatrix} = \begin{bmatrix} cos\ \theta & sin\theta & 1 \\ cos\left(\theta - \frac{2\pi}{3}\right) & sin\left(\theta - \frac{2\pi}{3}\right) & 1 \\ cos\left(\theta + \frac{2\pi}{3}\right) & sin\left(\theta + \frac{2\pi}{3}\right) & 1 \end{bmatrix} \begin{bmatrix} d \\ q \\ 0 \end{bmatrix} \tag{17}$$

2.3.2 Zero Sequence Controllers

The improved composite algorithm surpasses the traditional one after an experimental comparison of the results. The testing of a model photovoltaic power grid-connected system shows that the combination of modular multi-level converter technology and a photovoltaic grid-connected system, incorporating composite proportional integral control and quasi-proportional resonant control algorithms, yields improved results and feasibility(17).

The simplified circuit is considered here for calculations. The converter voltages are derived by applying Kirchhoff's Law.

$$V_r = \ V_{rg}\ + j i_r \omega L_f + V_z \tag{18}$$

$$V_y = \ V_{yg}\ + j i_y \omega L_f + V_z \tag{19}$$

$$V_b = \ V_{bg}\ + j i_b \omega L_f + V_z \tag{20}$$

Where V_a , $V_b\ and\ V_c$ is the output voltage of Cascaded MMC and i_r, i_y and i_b are the balanced currents supplied to a balanced network.

The Cascaded MMC has a nearly sinusoidal waveform. Hence the voltage drops across the inductor are considered negligible and are omitted from the above equations. Assuming the following ideal three-phase grid currents in phase with the grid phase voltage(18), the current in each phase is given as,

$$i_r = I_r sin(\omega_g t) = I_g sin(\omega_g t) \tag{21}$$

$$i_y = I_y sin\left(\omega_g t - \frac{2\pi}{3}\right) = I_g sin\left(\omega_g t - \frac{2\pi}{3}\right) \tag{22}$$

$$i_b = I_b sin\left(\omega_g t - \frac{2\pi}{3}\right) = I_g sin\left(\omega_g t - \frac{2\pi}{3}\right) \tag{23}$$

Where $I_r = I_y = I_b = I_g$ is taken for calculation by considering the balanced current injected into the balanced grid. ω_g is the grid frequency I_g is the grid current amplitude 19[19].

The apparent power in each phase of the converter is

$$S_r = V_r I_r^* = V_a I_g^* = P_r + jQ_r = P_g + jQ_g + P_{rz} + jQ_{az} \tag{24}$$

$$S_y = V_y I_y^* = V_y I_g^* = P_y + jQ_y = P_g + jQ_g + P_{yz} + jQ_{yz} \tag{25}$$

$$S_b = V_b I_b^* = V_b I_g^* = P_b + jQ_b = P_g + jQ_g + P_{bz} + jQ_{bz} \tag{26}$$

Where S_r, S_y and S_b are the apparent power in the r, y, and b phases. $P_r P_y$ and P_b are the active power supplied to the grid. Q_r, Q_y and Q_b are the reactive power supplied to the grid. Similarly, P_{rz}, P_{yz}, P_{bz}, Q_{rz}, Q_{yz} and Q_{bz} are the active and reactive power supplied by ZSV. The active power is alone considered[20]. P_g is the balanced power supplied to the grid. V_z balances the active power in the network by redistribution of power among the phases from one phase to the other. It does not supply extra power to the grid. Therefore, the total power supplied by zero sequence voltage and current should be zero i.e. P_{rz} $+P_{yz}$ + P_{bz} = 0.

The apparent power is derived in Equations (24) and (25) and Equation (26). The active power equations can be written as

$$P_r = P_g + P_{rz} \tag{27}$$

$$P_y = P_g + P_{yz} \tag{28}$$

$$P_b = P_g + P_{bz} \tag{29}$$

By solving Equations (27) and (28) and Equation (29) the average power P_g can be written as[21]

$$P_g = \frac{P_r + P_y + P_b}{3} \tag{30}$$

The active power supplied by a ZSV in all three phases can be calculated from equations such as,

$$P_{rz} = P_r - P_g = \frac{2P_a - P_y - P_b}{3} \tag{31}$$

$$P_{yz} = P_y - P_g = \frac{2P_y - P_r - P_b}{3} \tag{32}$$

$$P_{bz} = P_b - P_g = \frac{2P_b - P_y - P_r}{3} \tag{33}$$

The above equations can also be represented in phasor form as

$$P_{rz} = Re\{V_z I_r^*\} = V_z I_g \cos\, \alpha \tag{34}$$

$$P_{yz} = Re\{V_z I_y^*\} = V_z I_g \cos\left(\alpha + 2\frac{\pi}{3}\right) \tag{35}$$

$$P_{bz} = Re\{V_z I_b^*\} = V_z I_g \cos\left(\alpha - 2\frac{\pi}{3}\right) \tag{36}$$

By comparing the equations, the zero sequence voltage and its phase is given as,

$$V_z = \frac{2}{3}\frac{V_g}{P_g cos\alpha}\sqrt{\left(P_r^2 + P_y^2 + P_b^2 - P_r P_y - P_y P_b - P_b P_r\right)} \tag{37}$$

$$\alpha = tan^{-1}\left(\frac{\sqrt{3\left(P_b - P_y\right)}}{2P_r + P_y + P_b}\right) \tag{38}$$

The instantaneous zero sequence voltage is

$$V_z^* = V_z \sin(\omega t + \alpha) \tag{39}$$

Where V_z is the magnitude of Zero Sequence voltage, ω is the angular frequency, t is the time and α is the angle between Zero sequence voltage V_z and grid voltage V_g. The design is simple with accessible to develop higher levels. However, its gate driver circuits are still interpreted considering the number related to access switches being depreciated. The pulse width modulation system operates over the multicarrier system to generate the power switch's gating signals[(22)].

3 Results and Discussion

The irradiance value considered for each array is 1000Wm^{-2}, which is operated at the temperature of 30° C. Figure 2 shows the V-I curve of a solar module at different temperatures.

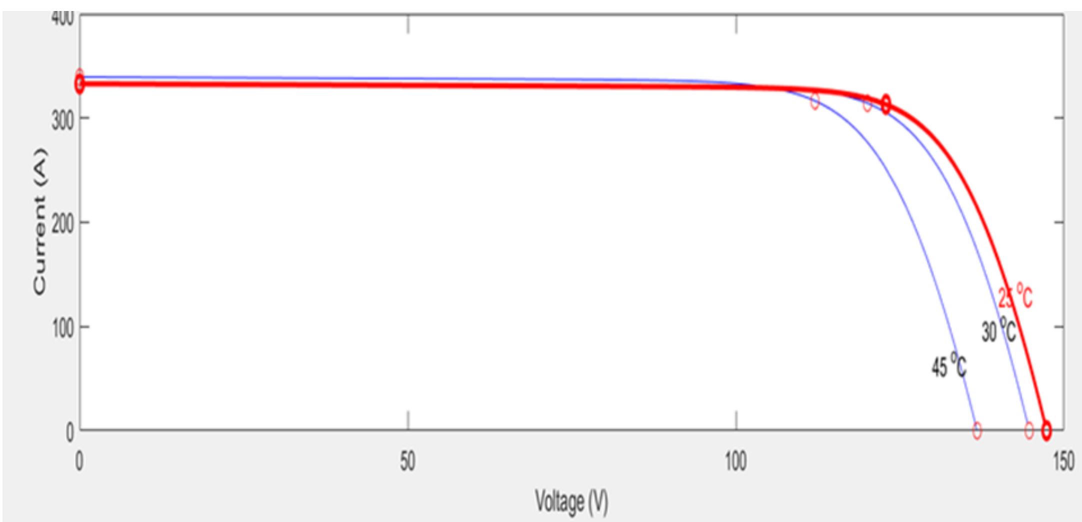

Fig 2. V-I curve at different temperatures

Several PV cells are connected in series to form a string. These strings are connected in parallel to form an array of PV modules. The solar module specifications are given in Table 1. These series and parallel configurations result in the increased output power of the system. The current and voltage is plotted for a solar array at different temperatures such as 25°C, 30°C, and 45 °C at constant irradiance of 1000 Wm^{-2}as shown in Figure 2.

Table 1. Solar Module Specifications

PARAMETERS	SYMBOL	VALUE	UNIT
Maximum Power	P_m	240	W
Open circuit voltage	V_{oc}	36.84	V
Short-circuit current	I_{sc}	8.32	A
Voltage at the maximum power point	V_{mp}	30.72	V
Current at the maximum power point	I_{mp}	7.83	A

At the Maximum PowerPoint, the maximum voltage obtained is 120V at 30°C. In each phase, three solar arrays are used. Therefore, in total for a phase system, nine solar arrays are connected. For each solar array, an MPPT module is connected. MPPT is used in each of the PV outputs to maintain the same voltage at partial shading. But when PV output is different for each panel of the same phase MPPT algorithm alone is not sufficient to maintain the voltage constant. Hence to maintain the voltage constant, a Zero sequence voltage controller is used.

The Zero Sequence controller system consists of a three-phase PLL, which is used to generate in-phase and quadrature components of the grid voltage. The MPPT controller generates the reference voltage of the PV panel which is compared to its actual counterpart and generates an axis current reference called i_d^*. The d-axis current is transformed to a stationary frame by multiplying with the in-phase component of the grid voltage unit vector that is sin θ.

Similarly, the quadrature component of the current in the stationary frame is obtained by multiplying q axis current (i_q^*) with the quadrature component of the grid voltage unit vector (cosθ). A Zero Sequence Voltage controller is used to generate voltage reference (V_g^*) of the converter. The vg is modified to generate a modulating signal which is then compared to phase-shifted carrier signals and gives a duty ratio for each sub-module. The output of the cascaded Modular Multilevel converter with seven-level output is shown in Figure 3 for each phase.

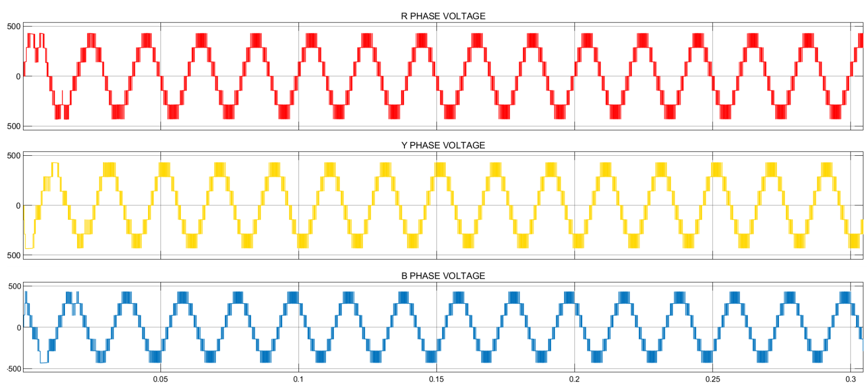

Fig 3. Seven Level Cascaded Modular Multilevel Converter Output

The output voltage generated by the converter at maximum is 430V. The output of the converter is passed through the inductor and capacitor to reduce the waveform distortion and provided to the grid. No additional filter circuit is needed. The output voltage waveform provided to the grid is shown in the maximum voltage produced is 360V. Figure 4 shows the Inverter voltage given to the grid after applying the inductor filter.

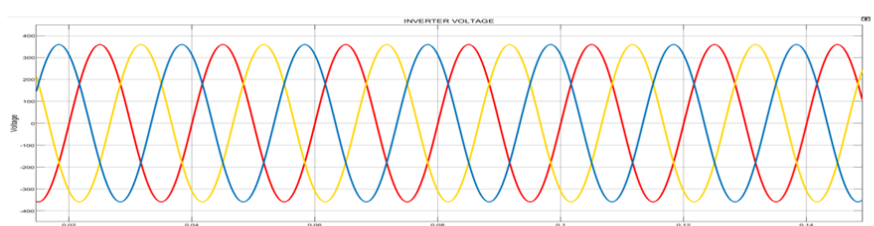

Fig 4. Inverter voltage

The maximum current produced is 40A. The proposed system provides a constant power of 20KW. Figure 5 represents the Inverter current provided to the grid. Figure 6 shows the real power produced by the proposed system.

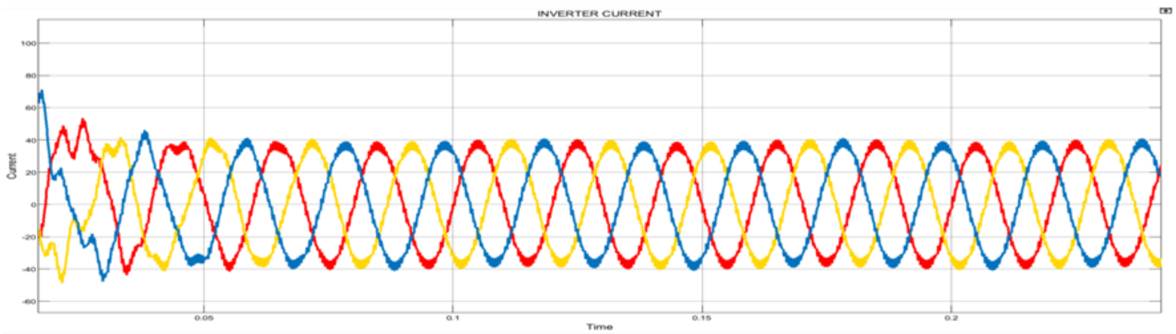

Fig 5. Inverter current

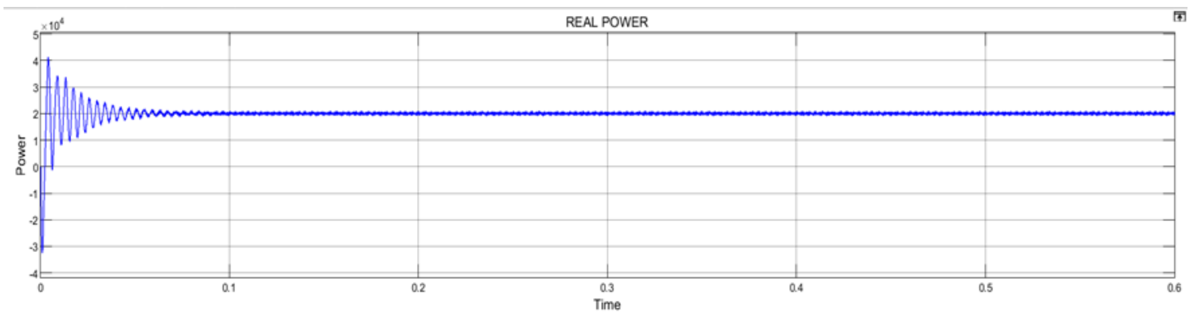

Fig 6. Real Power

The simulated results obtained for t phase voltage for the inverter and the grid voltage are synchronized in frequency and phase angle, as shown in Figure 7. Also, the inverter current is in phase with the grid phase voltage, as shown in Figure 8 which means the power is injected with the unity power factor.

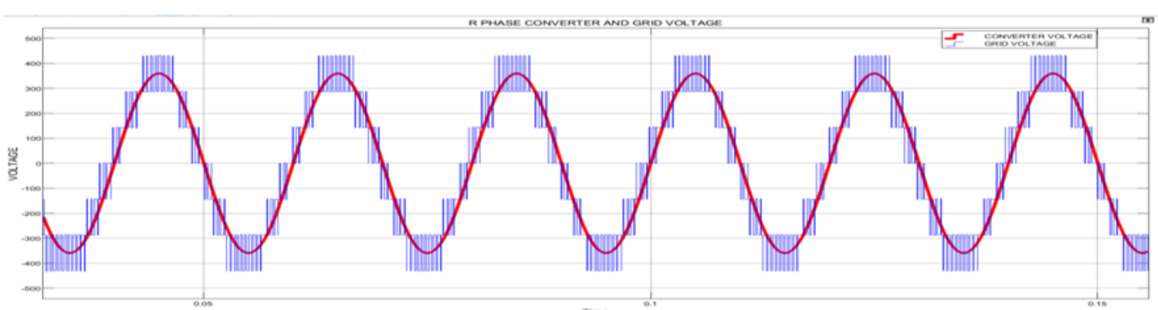

Fig 7. Converter phase voltage and Grid Voltage

The consequence is mainly heat losses in the cables of the electrical grid due to the harmonic irregularities when power is consumed. Hence, THD analysis is crucial for maintaining and enhancing power system stability. Figure 9 shows the current harmonics produced is 1.36 for the proposed system. Phase Shifted PWM (PS-PWM) technique provides less total harmonic distortion than the level-shifted PWM method. Total Harmonic distortion produced is 1.56% in the existing literature and the proposed system produces less total harmonic distortion of about 1.36%.

The total harmonics Distortion for inverter current is 1.36%. as shown in Figure 9 for the proposed seven-level cascaded Modular Multilevel Converter.

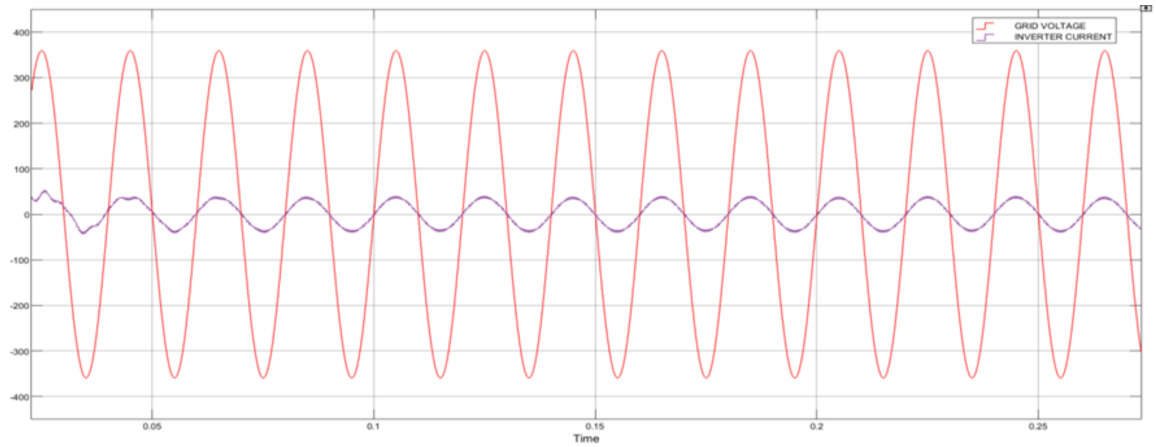

Fig 8. Grid Voltage and Inverter Current

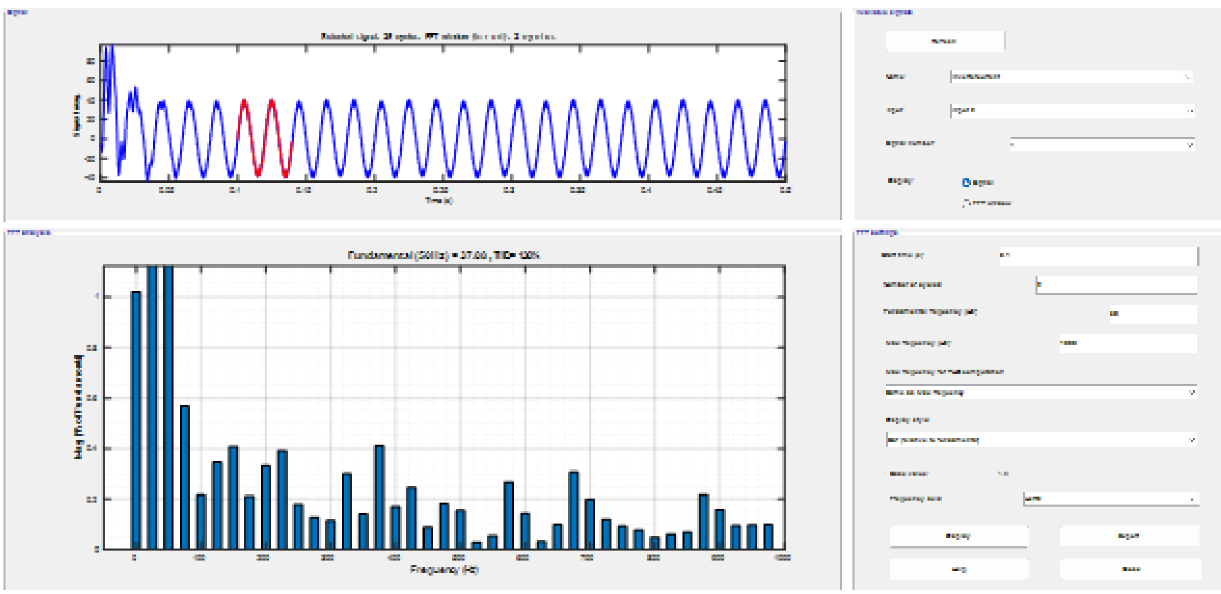

Fig 9. Total Harmonic Distortion of Current

4 Conclusion

The operation of grid-connected solar PV fed Converter topology during unbalanced power generation among the phases of the converter has been analyzed. The Zero Sequence Voltage can inject balance power into the grid during different partial shading conditions. The distributed MPPT algorithm is utilized here for balancing the power unbalances within the phases. Existing literature uses a two-stage conversion system, which has a DC-DC converter and a DC-AC converter for PV power generation. In the proposed work, single-stage conversion is used. It reduces the number of components used compared to two-stage conversion and so minimum power losses are produced. The single-stage conversion ensures reduced cost and improved reliability. Maximum power extraction from the PV module is achieved using the single-stage conversion and distributed MPPT.

The overall control circuitry with the converter model can mitigate the unbalanced-related power quality issues during varying irradiance. The converter topology with the Zero sequence controller is validated through simulation results in MATLAB SIMULINK software. It is important to mention that the converter model can also be utilized for more power generation by adding more PV Panels in the system. Moreover, the zero-sequence converter is used for active power compensation. In the future, reactive power compensation can be implemented. Energy Storage systems using batteries may also be included in the future.

References

1) Khemili FZ, Bouhali O, Lefouili M, Chaib L, El-Fergany AA, Agwa AM. Design of cascaded multilevel inverter and enhanced MPPT method for large-scale photovoltaic system integration. . *Sustainability*. 2023;15:9633–9633. Available from: https://doi.org/10.3390/su15129633.
2) Bagi SM, Kudchi FN, Bagewadi S. Power quality improvement using a shunt active power filter for grid connected photovoltaic generation system. In: IEEE Bangalore Humanitarian Technology Conference. IEEE. 2020;p. 1–4. Available from: https://doi.org/10.1109/B-HTC50970.2020.9298001.
3) Kulkarni J, Kumar N, Singh B. Control and Design of Seven-Level Cascaded Multilevel Converter for Transformerless Large-Scale Photovoltaic Integration. *J Inst Eng India Ser B*. 2020;101:623–629. Available from: https://doi.org/10.1007/s40031-020-00472-7.
4) Elsanabary A, Mekhilef S, Seyedmahmoudian M, Stojcevski A. An energy balancing strategy for modular multilevel converter based grid-connected photovoltaic systems. *IET Power Electron*. 2021;14:2115–2126. Available from: https://doi.org/10.1049/pel2.12113.
5) Vijeh M, Rezanejad M, Samadaei E, Bertilsson K. A general review of multilevel inverters based on main submodules: Structural point of view. *IEEE Transactions on Power Electronics*. 2019;34(10):9479–502. Available from: https://doi.org/10.1109/TPEL.2018.2890649.
6) Haq S, Biswas SP, Hosain MK, Rahman MA, Islam MR, Jahan S. A modular multilevel converter with an advanced PWM control technique for grid-tied photovoltaic system. . *Energies*. 2021;14:331–331. Available from: https://doi.org/10.3390/en14020331.
7) Alotaibi S, Darwish A. Modular multilevel converters for large-scale grid-connected photovoltaic systems: A review. . *Energies*. 2019;14:6213–6213. Available from: https://doi.org/10.3390/en14196213.
8) Parimalasundar E, Kumar NM, Geetha P, Suresh K. Performance investigation of modular multilevel inverter topologies for photovoltaic applications with minimal switches. *Electrical Engineering & Electromechanics*. 2022;6:28–34. Available from: https://doi.org/10.20998/2074-272X.2022.6.05.
9) Marzo I, Sanchez-Ruiz A, Barrena JA, Abad G, Muguruza I. Power balancing in cascaded H-bridge and modular multilevel converters under unbalanced operation: A review. *IEEE access*. 2009;9:110525–110568. Available from: https://doi.org/10.1109/ACCESS.2021.3103337.
10) Mishra PK, Tiwari P. Incremental conductance MPPT in grid connected PV system. *International Journal of Engineering, Science and Technology*. 2009;13(1):138–183. Available from: https://doi.org/10.4314/ijest.v13i1.21S.
11) Motahhir S, Hammoumi E, A, Ghzizal E, A. The most used MPPT algorithms: Review and the suitable low-cost embedded board for each algorithm. *Journal of cleaner production*. 2020;246:118983–118983. Available from: https://doi.org/10.1016/j.jclepro.2019.118983.
12) Umadevi C, Sundari MG, Karuvelam PS. Cascaded Fuzzy Logic Controlled Modular Multilevel Converter for PV Based DSTATCOM Applications. *J Electr Eng Technol*. 2024;19:1551–1563. Available from: https://doi.org/10.1007/s42835-023-01663-0.
13) Elsanabary AI, Konstantinou G, Mekhilef S, Townsend CD, Seyedmahmoudian M, Stojcevski A. Medium voltage large-scale grid-connected photovoltaic systems using cascaded H-bridge and modular multilevel converters: A review. *IEEE Access*. 2020;8:223686–99. Available from: https://doi.org/10.1109/ACCESS.2020.3044882.
14) Engin BM. Comprehensive review on distributed maximum power point tracking: Submodule level and module level MPPT strategies. *Solar Energy*. 2022;241:85–108. Available from: https://doi.org/10.1016/j.solener.2022.05.039.
15) Barcellona S, Barresi M, Piegari L. MMC-Based PV Single-Phase System with Distributed MPPT. *Energies*;13(15):3964–3964. Available from: https://doi.org/10.3390/en13153964.
16) Elmelegi A, Aly M, Ahmed EM, Alharbi AG. A simplified phase-shift PWM-based feedforward distributed MPPT method for grid-connected cascaded PV inverters. . *Solar Energy*. 2019;187:1–2. Available from: https://doi.org/10.1016/j.solener.2019.05.021.
17) Mansouri N, Lashab A, Sera D, Guerrero JM, Cherif A. Large photovoltaic power plants integration: A review of challenges and solutions. . *Energies*. 2019;12:3798–3798. Available from: https://doi.org/10.3390/en12193798.
18) Xie J. Application of optimized photovoltaic grid-connected control system based on modular multilevel converters. *Energy Inform*. 2024;7(24). Available from: https://doi.org/10.1186/s42162-024-00317-3.
19) Raziq H, Batool M, Riaz S, Afzal F, Akgül A. Power quality improvement of a distribution system integrating a large scale solar farm using hybrid modular multilevel converter with ZSV control. *Ain Shams Engineering Journal*. 2023;14(7). Available from: https://doi.org/10.1016/j.asej.2023.102218.
20) Sharma R, Das A. Enhanced active power balancing capability of grid-connected solar PV fed cascaded H-bridge converter. *IEEE Journal of Emerging and Selected Topics in Power Electronics*. 2019;7(4):2281–91. Available from: https://doi.org/10.1109/jestpe.2019.2890984.
21) Raziq H, Batool M, Riaz S, Afzal F, Akgül A, Riaz MB. Power quality improvement of a distribution system integrating a large scale solar farm using hybrid modular multilevel converter with ZSV control. *Ain Shams Engineering Journal*. 2023;14(7):102218–102218. Available from: https://dx.doi.org/10.1016/j.asej.2023.102218.
22) Alotaibi S, Darwish A. Modular Multilevel Converters for Large-Scale Grid-Connected Photovoltaic Systems: A Review. *Energies*. 2021;14(19):6213–6213. Available from: https://dx.doi.org/10.3390/en14196213.